

Relaxation of relativistic pair plasma in a massive photon field

Usman Shazad ^{1,†} and M. Iqbal¹

¹Department of Physics, University of Engineering and Technology, Lahore 54890, Pakistan

(Received 29 May 2023; revised 15 September 2023; accepted 18 September 2023)

The relaxation of relativistic hot electron–positron plasma is investigated by incorporating the effect of non-zero photon mass, and a quadruple Beltrami (QB) relaxed state for the magnetic vector potential is derived. The QB state is a linear superposition of four single force-free fields and is characterized by four self-organized structures of different length scales. The analysis of QB states shows that for certain values of generalized helicities at lower relativistic temperatures, plasma shows diamagnetic behaviour. It is also noteworthy that the inclusion of non-zero photon mass naturally provides the possibility of multiscale structure formation in the relaxed state. In this scenario, one of the field structures is significantly larger than the Compton wavelength of photons, while the other three structures are on the scale of the electron skin depth. The potential implications of this QB state for astrophysical environments are also discussed.

Key words: astrophysical plasmas, plasma properties

1. Introduction

Plasmas composed of relativistic electrons and positrons, also called pair plasmas, have garnered considerable interest due to their applicability in a variety of astrophysical and laboratory environments. Examples of this include accretion disks (Liang 1979; White & Lightman 1989; Björnsson *et al.* 1996), models of the early universe (Gibbons, Hawking & Siklos 1983; Tajima & Taniuti 1990), active galactic nuclei (AGN) (Lightman & Zdziarski 1987), pulsar magnetospheres (Curtis 1991; Istomin & Sobyenin 2007), hypothetical quark stars (Usov 1998) and in the laboratory recently, Sarri *et al.* (2015) created ion-free electron–positron (EP) plasma by using a compact laser-driven set-up. The existence of a variety of nonlinear structures such as waves, solitons and instabilities is well established in these relativistic EP plasmas. Aside from this, magnetic self-organization or relaxation is another important phenomenon in magnetized laboratory and astrophysical plasmas. During the process of plasma relaxation, a plasma attains an equilibrium state by minimizing its energy under some topological constraints. This equilibrium state is called a relaxed or self-organized state. In the case of ideal magnetohydrodynamics (MHD), the relaxed state can be obtained by minimizing the magnetic energy subject to the magnetic

[†] Email address for correspondence: usmangondle@gmail.com

helicity constraint. Specifically, the relaxed state corresponds to a single Beltrami field (a vector field whose vortex is collinear to itself) or state, which can be mathematically expressed as $\nabla \times \mathbf{B} = \lambda \mathbf{B}$, where \mathbf{B} denotes the magnetic field, λ is a constant, and the eigenvalue of the curl operator is referred to as the scale parameter. This single Beltrami relaxed state is force-free, flowless and devoid of pressure gradients. It is noteworthy that the entirety of the relaxed state structure's information, which includes its dimensions, nature, and shear or twist, is encompassed within λ (Woltjer 1958; Taylor 1974).

Later, to obtain a more realistic and non-force-free relaxed state, Hall MHD (HMHD) was invoked instead of ideal MHD. For HMHD, the relaxed state is the double Beltrami (DB) state, which is the superposition of two single force-free states. The DB state is characterized by two scale parameters, and it also shows a strong magnetofluid coupling resulting in significant pressure gradients (Mahajan & Yoshida 1998; Steinhauer 2002). In further studies, it was shown that the inertia of plasma species plays a significant role in the formation of multi-Beltrami relaxed state structures (Mahajan & Lingam 2015). In this regard, the relaxed state of an EP plasma is the triple Beltrami (TB) state. A TB state is a linear combination of three single Beltrami fields and is characterized by three scale parameters (Bhattacharyya, Janaki & Dasgupta 2003). While for a three-component plasma and when all the plasma species are inertial, the self-organized state is the quadruple Beltrami (QB) state – a linear combination of four single Beltrami fields with four self-organized structures (Shatashvili, Mahajan & Berezhiani 2016). In recent years, such multi-Beltrami relaxed states have also been investigated by several researchers in relativistic hot EP (Iqbal, Berezhiani & Yoshida 2008), relativistic hot electron–positron–ion (EPI) (Iqbal & Shukla 2012, 2013; Shazad, Iqbal & Ullah 2021; Shazad & Iqbal 2023), relativistic degenerate EPI (Shatashvili *et al.* 2016) and relativistic degenerate two electron-temperature electron–ion plasmas (Shatashvili, Mahajan & Berezhiani 2019).

The Beltrami states discussed above have also proven to be efficacious in plasma confinement (Mahajan & Yoshida 1998) and the modelling of various aspects of magnetized plasmas in astrophysical phenomena. Some applications of Beltrami states in astrophysical phenomena are solar flares (Ohsaki *et al.* 2002; Kagan & Mahajan 2010), solar arcades and loops (Bhattacharyya *et al.* 2007; Fuentes-Fernández, Parnell & Hood 2010), coronal heating (Mahajan *et al.* 2001; Browning & Van der Linden 2003), large-scale dynamo and reverse dynamo mechanisms (Mininni, Gómez & Mahajan 2002; Mahajan *et al.* 2005; Kotorashvili, Revazashvili & Shatashvili 2020; Kotorashvili & Shatashvili 2022), turbulence (Krishan 2004; Krishan & Mahajan 2004) and striped wind of pulsar nebula (Pino, Li & Mahajan 2010). Furthermore, the application of Beltrami states has also been expanded to encompass curved space–time, allowing for their utilization in the modelling of plasmas located in the vicinity of black holes as well as the early universe (Bhattacharjee *et al.* 2015; Bhattacharjee, Feng & Stark 2018; Asenjo & Mahajan 2019; Bhattacharjee 2020; Bhattacharjee & Feng 2020).

Recent years have seen a number of studies exploring the nonlinear interaction between photons and relativistic hot EP plasmas (Tajima & Taniuti 1990; Shukla 1993; Shukla, Tsintsadze & Tsintsadze 1993; Mendonça & Shukla 2008). However, the goal of the present work is to investigate the relaxation of relativistic EP plasma that is composed of inertial relativistic hot electrons and positrons in a massive photon field. Moreover, it is also crucial to mention that only relativistic temperature effects will be taken into account in this study. A plasma is considered relativistically hot if the thermal energy possessed by plasma particles is equal to or surpasses their rest mass energy. In the context of our plasma model it is important to explain that in classical electrodynamics, the photon is assumed to have zero mass (Goldhaber & Nieto 1971; Tu, Luo & Gillies 2005; Goldhaber & Nieto

2010; Jackson 2021). It is deduced from the condition that the Lagrangian describing the electromagnetic field must have gauge invariance. In the same vein as the cosmological constant and the masses of neutrinos, both of which were originally considered to be precisely zero until empirical evidence revealed otherwise, it is plausible to presume that a photon possesses a mass that is very small but not zero (Reece 2019; Aghanim *et al.* 2020). Research on dark matter, in which massive dark photons are postulated to be force carriers that can kinetically interact with the photon predicted by the standard model, is another factor that continues to pique interest in massive photons (Filippi & De Napoli 2020).

The electromagnetic field Lagrangian, first considered by Proca and also termed the Proca Lagrangian, can be modified to incorporate a mass term to account for photon mass that can be expressed as (Jackson 2021)

$$L_{\text{Proca}} = \frac{1}{8\pi\lambda_p^2} A_\mu A^\mu - \frac{1}{c} J_\mu A^\mu - \frac{1}{16\pi} F_{\mu\nu} F^{\mu\nu}, \tag{1.1}$$

where A_μ , J_μ , $F_{\mu\nu}$, c and λ_p ($h/m_\nu c$, in which h is Planck’s constant and m_ν is photon mass) are four potentials, four currents, electromagnetic field stress tensor, the speed of light and the Compton wavelength, respectively. This Proca Lagrangian leads to the following equation of motion for massive photons:

$$\partial_\nu F_{\mu\nu} + \frac{1}{\lambda_p^2} A_\mu = \frac{4\pi}{c} J_\mu. \tag{1.2}$$

Some of the immediate repercussions of non-zero photon mass include wavelength dependence of the speed of light, departures from the exactness of Coulomb’s and Ampere’s laws, longitudinal polarization of electromagnetic waves, and Yukawa-like dependency of the magnetic field formed by a magnetic dipole (Goldhaber & Nieto 1971; Bay & White 1972; Rawls 1972; Tu *et al.* 2005; Goldhaber & Nieto 2010). Similarly, a very important implication of non-zero photon mass is a modification of Ampere’s law. For instance, Ampere’s law in Maxwell–Proca electrodynamics can be expressed as (Ryutov 1997)

$$\nabla \times \mathbf{B} + \frac{\mathbf{A}}{\lambda_p^2} = \frac{4\pi}{c} \mathbf{J} + \frac{1}{c} \frac{\partial \mathbf{E}}{\partial t}, \tag{1.3}$$

where \mathbf{B} , \mathbf{E} , \mathbf{A} and \mathbf{J} are magnetic field, electric field, vector potential and current density, respectively. Due to their extreme precision, photon mass measurements in laboratories have reached their limitations (Tu & Luo 2004). The currently recognized upper limit for photon mass is $m_\nu \leq 10^{-49}$ g and corresponding to this value $\lambda_p \geq 1$ au (Adelberger, Dvali & Gruzinov 2007; Particle Data Group 2022). Recently, in the context of magnetized plasmas, some specific solutions to the MHD equations that take into consideration the finite photon mass have been presented and studied in light of the prospect of refining the estimate of the photon mass based on a variety of astrophysical observations (Ryutov 1997, 2007, 2009, 2010). Moreover, Ryutov, Budker & Flambaum (2019) have also investigated the MHD plasma equilibrium to study the effect of Maxwell–Proca electromagnetic stresses on galactic rotation curves (Ryutov *et al.* 2019). The study also suggests that standard theory of plasma relaxation (Woltjer 1958; Taylor 1974) can also be extended to such plasma systems which incorporate the effect of non-zero photon mass, and for such plasma models magnetic vector potential \mathbf{A} also satisfies the Beltrami condition $\nabla \times \mathbf{A} = \lambda \mathbf{A}$. Bhattacharjee (2023) has recently advanced the concept of equilibrium states in terms of vector potential and obtained a TB state for a quasineutral single species plasma.

Due to the ubiquity of EP plasmas and their inherent self-organizing nature, which leads to the formation of coherent magnetic and flow patterns, it becomes crucial to investigate the plasma equilibria of relativistic hot EP plasmas. In the present work, a QB relaxed state equation for magnetic vector potential in relativistic hot EP plasma is derived by incorporating the effect of non-zero photon mass by considering it as a mobile fluid. The objective of this study is to examine the potential presence of Beltrami states at scales larger than the Compton wavelength and explore the variations that arise as a result of a non-zero photon mass. In contrast to the Beltrami state applicable to zero photon mass, the states under consideration predominantly involve the magnetic vector potential \mathbf{A} due to its dynamic nature within the framework of massive electromagnetism. This study aims to address certain analytical challenges in the field of massive electromagnetism, specifically related to multi-Beltrami equilibria such as the upper mass limit for photons and galactic rotation curves.

To derive a QB relaxed state, first, vortex dynamics equations for pair species are derived from relativistic equations of motion, and then the steady-state solutions of vortex dynamics equations are coupled with a modified Ampere's law. This modified Ampere's law incorporates the effect of non-zero photon mass in Maxwell-Proca electrodynamics. Furthermore, the analysis of the relaxed state shows that all the scale parameters become real for higher relativistic temperatures and sub-Alfvénic flows of plasma species. These scale parameters also show the possibility of multiscale structure formation in this QB state. The size of one of the structures is greater than or equal to the Compton wavelength. While the size of one structure is greater than the electron skin depth, the dimensions of the remaining two structures are equal to or smaller than the electron skin depth. Additionally, an analytical solution of the QB field and flow is presented in an axisymmetric cylindrical geometry. The field profiles show that at lower relativistic temperatures, for given values of generalized helicities of plasma species, plasma shows a diamagnetic trend. Also, the field and flow profiles show the possibility for the formation of microscale energy reservoirs, which may be either kinetic or magnetic in nature. The existence of microscale energy reservoirs can be attributed to the multiscale structures present in the QB state, which have important implications for dynamo and reverse dynamo processes.

This paper is structured in the following manner. In § 2, from model equations, the QB relaxed state equation is derived. The general properties of the QB self-organized state are presented in § 3. In § 4, the analytical solution of the QB field and flow in an axisymmetric cylindrical geometry is presented. The summary of the present findings is given in § 5.

2. Model equations and the QB state

Consider a quasineutral and incompressible magnetized relativistic hot EP plasma in a massive photon field. In order to account for the effect of non-zero mass, we will use Maxwell-Proca electrodynamics. Now the continuity equation and relativistic equation of motion for α (electrons, e; positrons, p) plasma species are

$$\frac{\partial n_\alpha}{\partial t} + \nabla \cdot (n_\alpha \mathbf{V}_\alpha) = 0, \quad (2.1)$$

$$\frac{\partial \mathbf{\Pi}_\alpha}{\partial t} + \frac{1}{n_\alpha} \nabla p_\alpha = q_\alpha \mathbf{E} + \mathbf{V}_\alpha \times \left(\mathbf{\Pi}_\alpha + \frac{q_\alpha}{c} \mathbf{B} \right), \quad (2.2)$$

where $\mathbf{\Pi}_\alpha = m_{0\alpha} \gamma_\alpha G_\alpha \mathbf{V}_\alpha$, $p_\alpha = n_\alpha T_\alpha / \gamma_\alpha$, n_α , $m_{0\alpha}$, \mathbf{V}_α , $\gamma_\alpha = 1/\sqrt{1 - (V_\alpha/c)^2}$, T_α and q_α are relativistic momentum, thermal pressure, number density, rest mass, velocity, relativistic Lorentz factor, temperature and electric charge of plasma species, respectively, while \mathbf{E} and \mathbf{B} are the electric and magnetic fields, c is the speed of light,

$G_\alpha(z_\alpha) = K_3(z_\alpha)/K_2(z_\alpha)$ in which $z_\alpha = m_{0\alpha}c^2/T_\alpha$ and K_2 and K_3 are MacDonald functions of second and third order (Berezhiani *et al.* 2002). The factor G_α accounts for the thermal relativistic effects of plasma species. The asymptotic approximation of G_α for non-relativistic temperatures is $G_\alpha = 1 + 5T_\alpha/2m_{0\alpha}c^2$, whereas, for ultrarelativistic temperatures of plasma species $G_\alpha = 4T_\alpha/m_{0\alpha}c^2$. In relativistic EP plasma $m_{0\alpha} = m_0$ and $q_\alpha = \pm e$, where m_0 and e are the rest mass of an electron and elementary charge, respectively. It is also important to mention that in this plasma model we will only consider the thermal relativistic effects, and the relativistic temperatures of both the plasma species are assumed equal ($G_\alpha = G$) while the relativistic streaming effects of plasma species are ignored, i.e. $\gamma_\alpha \approx 1$. Additionally, the equation of motion (2.2) is augmented with the following adiabatic equation of state:

$$\frac{n_\alpha z_\alpha}{\gamma_\alpha K_2(z_\alpha)} \exp[-z_\alpha G_\alpha(z_\alpha)] = \text{constant}. \tag{2.3}$$

When considering the non-relativistic limit, (2.3) produces the typical outcome for a monoatomic ideal gas ($n_\alpha/\gamma_\alpha T_\alpha^{3/2} = \text{constant}$). On the other hand, when examining the ultrarelativistic limit, the equation of state for the photon gas is obtained ($n_\alpha/\gamma_\alpha T_\alpha^3 = \text{constant}$).

In order to express model equations in dimensionless form, we will use the electron skin depth ($\lambda_e = \sqrt{m_0c^2/8\pi n_0e^2}$, where n_0 is plasma species density in the rest frame), Alfvén speed ($v_A = B_0/(8\pi m_0n_0)^{1/2}$), some arbitrary magnetic field B_0 , and λ_e/v_A to normalize length, plasma species velocities, magnetic field and time, respectively. Now, from (2.2) along with relations $\mathbf{E} = -\nabla\phi - c^{-1}\partial\mathbf{A}/\partial t$ and $\mathbf{B} = \nabla \times \mathbf{A}$, the normalized equations of motion for electron and positron species are

$$\frac{\partial \mathbf{\Pi}_e}{\partial t} = \mathbf{V}_e \times \mathbf{\Omega}_e - \nabla \Psi_e, \tag{2.4}$$

$$\frac{\partial \mathbf{\Pi}_p}{\partial t} = \mathbf{V}_p \times \mathbf{\Omega}_p - \nabla \Psi_p, \tag{2.5}$$

where $\mathbf{\Pi}_{e,p} = G\mathbf{V}_{e,p} \mp \mathbf{A}$, $\mathbf{\Omega}_{e,p} = \nabla \times G\mathbf{V}_{e,p} \mp \mathbf{B}$, $\Psi_{e,p} = c_A^2 G \pm \phi$, $c_A = c/v_A$ and ϕ is scalar electric potential. In the above equations $\mathbf{\Pi}_\alpha$ is generalized or canonical momentum while $\mathbf{\Omega}_\alpha$ is generalized or canonical vorticity of plasma species. In order to incorporate the effect of photon mass and couple the independent dynamics of plasma species, we employ Ampere’s law, as expressed in (1.3), while assuming that displacement currents can be neglected due to the non-relativistic directed flow velocities ($\gamma_{e,p} \approx 1$) of the plasma species. In normalized form, it can be expressed as

$$\nabla \times \mathbf{B} + \frac{\lambda_e^2}{\lambda_p^2} \mathbf{A} = \frac{1}{2}(\mathbf{V}_p - \mathbf{V}_e). \tag{2.6}$$

As mentioned earlier, $\lambda_p = h/m_v c$, and in this study we will use $m_v \leq 10^{-49}$ g and corresponding to this value, $\lambda_p \geq 1$ au (Adelberger *et al.* 2007). It is important to note that in massive electromagnetism, \mathbf{A} and ϕ are observable quantities that effect the dynamics of plasma and also satisfy the following Lorentz condition:

$$\nabla \cdot \mathbf{A} + \frac{1}{c} \frac{\partial \phi}{\partial t} = 0. \tag{2.7}$$

We can now obtain the vortex evolution equations for plasma species by taking the curl of the equations of motion ((2.4)–(2.5))

$$\frac{\partial \boldsymbol{\Omega}_e}{\partial t} = \nabla \times (\mathbf{V}_e \times \boldsymbol{\Omega}_e), \quad (2.8)$$

$$\frac{\partial \boldsymbol{\Omega}_p}{\partial t} = \nabla \times (\mathbf{V}_p \times \boldsymbol{\Omega}_p). \quad (2.9)$$

From (2.8)–(2.9), it is also evident that there is no role for gradient terms in vortex evolution. The steady-state solution of the vortex dynamics equations gives the following two equations:

$$\boldsymbol{\Omega}_e = aG\mathbf{V}_e, \quad (2.10)$$

$$\boldsymbol{\Omega}_p = bG\mathbf{V}_p, \quad (2.11)$$

where a and b are called Beltrami parameters. It is also essential to highlight that (2.10)–(2.11) are also steady-state solutions of equations of motion (2.4)–(2.5) provided the gradient terms vanish independently ($\nabla \Psi_{e,p} = 0$). The condition $\nabla \Psi_{e,p} = 0$, provides Bernoulli's condition ($\Psi_{e,p} = \text{constant}$), whereas the condition, in which generalized vorticities are aligned with flows ($\boldsymbol{\Omega}_\alpha \parallel \mathbf{V}_\alpha$), is known as the Beltrami condition. The equilibrium state described by these Beltrami and Bernoulli conditions is referred to as the Beltrami–Bernoulli equilibrium state. So the Beltrami–Bernoulli conditions ($\boldsymbol{\Omega}_\alpha \parallel \mathbf{V}_\alpha$ and $\Psi_{e,p} = \text{constant}$), in conjunction with Ampere's law, equation of state (2.3) and continuity equation (2.1), constitute a comprehensive equilibrium system that can be used to determine fields and flows. It is also worth noting that for steady-state (i.e. for constant density) continuity equations ($n_\alpha \nabla \cdot \mathbf{V}_\alpha = 0$) for plasma species, the incompressibility conditions for magnetic field and flow are inherently satisfied by the Beltrami conditions (Berezhiani, Shatashvili & Mahajan 2015) which also lead to conservation of generalized vorticities of plasma species ($\nabla \cdot \boldsymbol{\Omega}_\alpha = 0$). Moreover, the Beltrami parameters (a and b) in (2.10)–(2.11) are linked with generalized helicities of plasma species, which are the ideal invariants of this plasma system. The equations of motion ((2.4)–(2.5)), Ampere's law (2.6) and vortex dynamics ((2.8)–(2.9)) yield three ideal invariants or constants of motion for this plasma model (Steinhauer & Ishida 1997; Mahajan & Lingam 2015), namely the generalized helicity of electron (h_e) and positron (h_p) species and magnetofluid energy (W) that can be expressed as

$$h_e = \frac{1}{2} \int_v (\boldsymbol{\Pi}_e \cdot \boldsymbol{\Omega}_e) dv, \quad (2.12)$$

$$h_p = \frac{1}{2} \int_v (\boldsymbol{\Pi}_p \cdot \boldsymbol{\Omega}_p) dv, \quad (2.13)$$

$$W = \frac{1}{2} \int_v \left(GV_e^2 + GV_p^2 + B^2 + \frac{\lambda_e^2}{\lambda_p^2} A^2 \right) dv, \quad (2.14)$$

where \int_v is a volume integral and dv is a volume element. It is also essential to note that the overall volumetric magnetic energy density in Proca electrodynamics exhibits a comparable characteristic to that of Maxwellian electrodynamics. Nevertheless, a deviation from the Maxwellian characteristic can be observed in the overall magnetic pressure within the framework of Proca electrodynamics. This deviation arises due to the negative contribution of the massive photon ($\lambda_e^2 A^2 / \lambda_p^2$) to this particular quantity.

Consequently, the plasma dynamics can undergo significant modifications due to the presence of negative Proca pressure, which exerts a force that pulls plasmas towards regions with higher magnetic field strength (Ryutov *et al.* 2019; Bhattacharjee 2023). In this study, we will focus only on Beltrami conditions ((2.10)–(2.11)) to derive an equilibrium state. But it is important to mention here that the variational technique is another approach to derive a relaxed state equation, in which the ideal invariants of the plasma system are minimized. Now, the functional to be minimized in order to obtain an equilibrium state can be written as

$$\delta (W - \chi_e h_e - \chi_p h_p) = 0, \tag{2.15}$$

where χ_e and χ_p are some arbitrary and real-valued constants. In the calculus of variation, these constants are called Lagrange multipliers. Upon setting the independent variations of δV_e , δV_p and δA equal to zero, a set of three equations ((2.6) and (2.10)–(2.11)) can also be retrieved.

Now, in order to derive an equation describing the relaxed state, we will simultaneously solve (2.6) and (2.10)–(2.11). From (2.6), substituting the value of V_e in (2.10), we get

$$V_e = \frac{2}{b - a} \left[(\nabla \times)^3 A - b (\nabla \times)^2 A + \left(\frac{1}{G} + \frac{\lambda_e^2}{\lambda_p^2} \right) \nabla \times A - \frac{b \lambda_e^2}{\lambda_p^2} A \right], \tag{2.16}$$

where $(\nabla \times)^3 = \nabla \times \nabla \times \nabla \times$ and $(\nabla \times)^2 = \nabla \times \nabla \times$. The expression for V_p can be obtained by substituting the value of V_e from (2.16) into (2.6), and it is given by

$$V_p = \frac{2}{b - a} \left[(\nabla \times)^3 A - a (\nabla \times)^2 A + \left(\frac{1}{G} + \frac{\lambda_e^2}{\lambda_p^2} \right) \nabla \times A - \frac{a \lambda_e^2}{\lambda_p^2} A \right]. \tag{2.17}$$

Also, the bulk fluid velocity V (where $V = 0.5[V_e + V_p]$) of plasma by using the values V_e and V_p from (2.16)–(2.17) in terms of A , can be expressed as

$$V = d_1 (\nabla \times)^3 A - d_2 (\nabla \times)^2 A + d_3 \nabla \times A - d_4 A, \tag{2.18}$$

where $d_1 = 2/(b - a)$, $d_2 = 0.5d_1(a + b)$, $d_3 = d_1(G^{-1} + \lambda_e^2 \lambda_p^{-2})$ and $d_4 = 0.5d_1 \lambda_e^2 \lambda_p^{-2}(a + b)$. It is also important to note that (2.16)–(2.18) demonstrate a clear indication of a robust coupling between the field and flow in the relaxed state. The equation for the relaxed state, expressed in terms of A , can be derived by replacing the value of V_e from (2.16) into (2.10), and it is given by

$$(\nabla \times)^4 A - k_1 (\nabla \times)^3 A + k_2 (\nabla \times)^2 A - k_3 \nabla \times A + k_4 A = 0, \tag{2.19}$$

where $(\nabla \times)^4 = \nabla \times \nabla \times \nabla \times \nabla \times$, $k_1 = a + b$, $k_2 = ab + G^{-1} + \lambda_e^2 \lambda_p^{-2}$, $k_3 = (a + b)(0.5G^{-1} + \lambda_e^2 \lambda_p^{-2})$ and $k_4 = ab \lambda_e^2 \lambda_p^{-2}$. The relaxed state of a relativistic hot pair plasma with non-zero photon mass, which is described by (2.19) in terms of A , is referred to as the QB state. The emergence of a QB state in this system can be attributed to the incorporation of inertia of electron and positron species with distinct generalized helicities of electrons and positrons (i.e. distinct Beltrami parameters a and b) and non-zero mass of mobile fluid photons. The theoretical framework of vortical dynamics considers the interaction between the magnetic field, flow and massive photon field as being of equal importance.

In this framework, the photon is conceptualized as a mobile fluid within the system. It is important to highlight that in Maxwellian electrodynamics, a photon has the potential to acquire an effective mass while it undergoes propagation within a plasma medium. Therefore, the formalism presented in this paper is based on the fundamental assumption that photons are a mobile fluid with a non-zero rest mass and that their dynamics can be derived from the Proca Lagrangian (Anderson 1963; Mendonça, Martins & Guerreiro 2000; Bhattacharjee 2023).

Additionally, by neglecting the mass of photons, the TB state, which has been the subject of investigation by Iqbal *et al.* (2008), can be derived. On the other hand, from the Beltrami conditions and Ampere's law, as described by (2.6) and (2.10)–(2.11), with the following assumptions: $a = b = \mu$ and $G = 1$, the resulting relaxed state equation is a TB state that is given by

$$(\nabla \times)^3 \mathbf{A} - \mu (\nabla \times)^2 \mathbf{A} + \left(\frac{\lambda_e^2}{\lambda_p^2} + 1 \right) \nabla \times \mathbf{A} - \frac{\mu \lambda_e^2}{\lambda_p^2} \mathbf{A} = 0. \quad (2.20)$$

So from TB equation (2.20) it is evident that when the same generalized helicities are used for both plasma species and non-relativistic regimes, the relaxed state of this plasma model seems to be the same as what Bhattacharjee (2023) found for non-relativistic single species quasineutral incompressible plasma.

3. General properties of the QB state

The QB state (2.19) can be expressed as the linear superposition of four distinct force-free Beltrami states and is characterized by four scale parameters (λ_j). These scale parameters are measures of shear or twist ($\lambda = \mathbf{J} \cdot \mathbf{B}/B^2$), while the inverse of them gives the size (dimensionally λ_j is equal to inverse of the length) of the relaxed state structures. Here, the commutative property of the curl operator allows us to write the QB equation (2.19) in terms of scale parameters in the following manner:

$$(\text{curl} - \lambda_1) (\text{curl} - \lambda_2) (\text{curl} - \lambda_3) (\text{curl} - \lambda_4) \mathbf{A} = 0. \quad (3.1)$$

From (3.1), the scale parameters (λ_j) can be related to the coefficients k_j of the QB equation (2.19) in the following way:

$$k_1 = \lambda_1 + \lambda_2 + \lambda_3 + \lambda_4, \quad (3.2)$$

$$k_2 = \lambda_1 \lambda_2 + \lambda_2 \lambda_3 + \lambda_1 \lambda_3 + \lambda_1 \lambda_4 + \lambda_2 \lambda_4 + \lambda_3 \lambda_4, \quad (3.3)$$

$$k_3 = \lambda_1 \lambda_2 \lambda_3 + \lambda_1 \lambda_2 \lambda_4 + \lambda_2 \lambda_3 \lambda_4 + \lambda_1 \lambda_3 \lambda_4, \quad (3.4)$$

$$k_4 = \lambda_1 \lambda_2 \lambda_3 \lambda_4. \quad (3.5)$$

These relations between λ_j and k_j also satisfy Vieta's formula, so the values of scale parameters are the roots of the following quartic equation:

$$\lambda^4 - k_1 \lambda^3 + k_2 \lambda^2 - k_3 \lambda + k_4 = 0. \quad (3.6)$$

The formulae for calculating the eigenvalues (λ_j) of the QB state from the quartic equation (3.6) are as follows:

$$\lambda_1 = \frac{k_1}{4} + \frac{M + N}{2}, \tag{3.7}$$

$$\lambda_2 = \frac{k_1}{4} + \frac{M - N}{2}, \tag{3.8}$$

$$\lambda_3 = \frac{k_1}{4} - \frac{M + O}{2}, \tag{3.9}$$

$$\lambda_4 = \frac{k_1}{4} - \frac{M - O}{2}, \tag{3.10}$$

where the values of M , N and O are given by

$$M = 0.5\sqrt{k_1^2 - 4k_2 + 4H}, \tag{3.11}$$

$$H = w_3^{-1}(w_3k_2 + 3k_1k_3 - 12k_4 - k_2^2 - (3k_3^2 + 3k_4k_1^2 - 12k_2k_4 - k_2^2)^2), \tag{3.12}$$

$$w_1 = \frac{9k_1k_2k_3 - 36k_4 - 2k_2^3 - k_3^2 - 27k_4k_1^2 + 108k_2k_4}{54}, \tag{3.13}$$

$$w_2 = \frac{3k_1k_3 - 12k_4 - k_2^2}{9}, \tag{3.14}$$

$$w_3 = \sqrt[3]{729 \left(w_1 + \sqrt{w_1^2 + w_2^3} \right)}, \tag{3.15}$$

whereas in the case of $M \neq 0$, N and O are given by

$$N = \sqrt{0.75k_1^2 - 2k_2 - M^2 + 0.25M^{-1}(4k_1k_2 - 8k_3 - k_1^2)}, \tag{3.16}$$

$$O = \sqrt{0.75k_1^2 - 2k_2 - M^2 - 0.25M^{-1}(4k_1k_2 - 8k_3 - k_1^2)}, \tag{3.17}$$

but when $M = 0$,

$$N = \sqrt{0.75k_1^2 - 2k_2 + 2\sqrt{H^2 - 4k_4}}, \tag{3.18}$$

$$O = \sqrt{0.75k_1^2 - 2k_2 - 2\sqrt{H^2 - 4k_4}}. \tag{3.19}$$

Equations (3.7)–(3.10) demonstrate that the eigenvalues are dependent on the plasma parameters, specifically the electron skin depth, Compton wavelength of photon, Beltrami parameters and relativistic temperatures of plasma species. The eigenvalues associated with this QB state are either real or a combination of two real and a pair of complex conjugate eigenvalues. One simple approach for conducting an analysis of the characteristics of scale parameters requires employing the discriminant (D) of the quartic equation (3.6). For example, when $D < 0$, two scale parameters are real and the other two are complex conjugate to each other. On the other hand, when $D > 0$, all of the scale parameters are either real or complex conjugate. More specifically, all the eigenvalues are real and distinct when $D > 0$, $S = 16k_1^2k_2 - 3k_1^4 - 16k_1k_3 - 16k_2^2 + 64k_4 < 0$ and

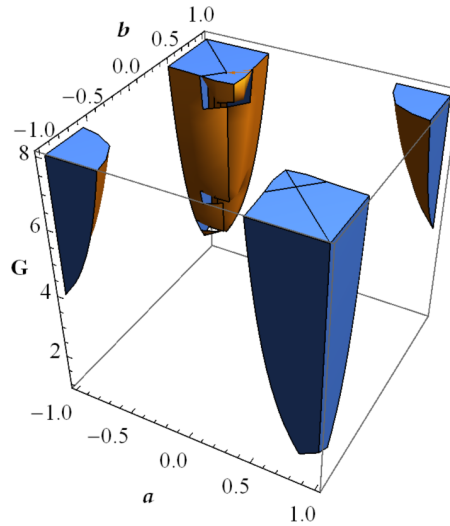


FIGURE 1. Nature of the eigenvalues of the QB state as a function of a , b and G . In the coloured region all the eigenvalues are real and distinct.

$T = 8k_2 - 3k_1^2 < 0$, but when D , S and T are greater than zero, there are two pairs of complex conjugate eigenvalues.

To see a glimpse of the character of scale parameters, the conditions $D > 0$, $S < 0$ and $T < 0$, have been plotted in figure 1 as a function of Beltrami parameters and thermal energy. In the coloured region, all the scale parameters are real, while in the transparent region, two scale parameters are complex conjugate to each other and the other two are real and distinct. Figure 1 demonstrates that for Alfvénic or super-Alfvénic flows of plasma species at lower relativistic temperatures, two scale parameters are real while the other two are complex conjugates. It is important to mention that the Beltrami parameters are basically the ratio between the flow vorticity modified magnetic field and the respective flow of plasma species ($|\mathbf{B} \pm \nabla \times G\mathbf{V}_\alpha|/|G\mathbf{V}_\alpha|$). So when $a, b \leq 1$, the flow is Alfvénic or super-Alfvénic, but when $a, b > 1$ the flow is sub-Alfvénic. Now, it can be seen from the plot when the flows become sub-Alfvénic and the relativistic temperature of plasma species increases, some of the complex eigenvalues become real. So from the plot, it can be concluded that at higher relativistic temperatures and for sub-Alfvénic flows, scale parameters are real and distinct. Corresponding to these real eigenvalues, the relaxed state shows a paramagnetic trend, whereas for the combination of real and complex eigenvalues, the plasma shows diamagnetic or partial diamagnetic behaviour.

Furthermore, in figure 2, we demonstrate the effect of relativistic temperature on the nature and variation in the sizes of scale parameters for fixed values of Beltrami parameters ($a = 1.0$ and $b = 2.0$) by plotting λ_j from (3.7)–(3.10). From the plot, it can be seen that when the plasma is non-relativistic, i.e. $G = 1$, there are only two real eigenvalues, while the other two are complex. The values of scale parameters are $\lambda_1 = 2.08 \times 10^{-12}$, $\lambda_{2,3} = 0.6032 \pm 0.6874i$ and $\lambda_4 = 1.794$. By increasing the relativistic temperature to $G = 2.65$, all the eigenvalues become real and have the following values: $\lambda_1 = 5.521 \times 10^{-12}$, $\lambda_2 = 0.5268$, $\lambda_3 = 0.5622$, and $\lambda_4 = 1.9109$. In the case of an ultrarelativistic regime, for instance, when $G = 8.0$, the eigenvalues have the following values: $\lambda_1 = 1.67 \times 10^{-11}$, $\lambda_2 = 0.1026$, $\lambda_3 = 0.9281$ and $\lambda_4 = 1.9693$. From figure 2 and the values of scale parameters for different relativistic temperatures, it is very clear that by increasing the

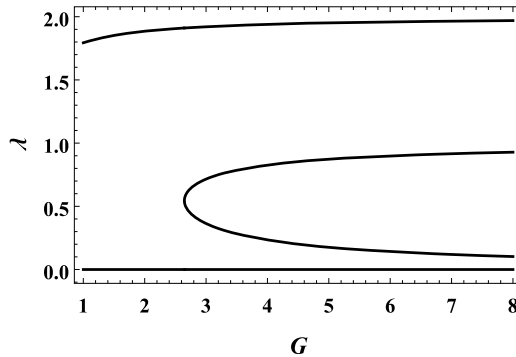


FIGURE 2. Character and variation in the sizes of the scale parameters as a function of thermal energy G for $a = 1.0$ and $b = 2.0$.

relativistic temperature, all the scale parameters become real and distinct, and the values of scale parameters λ_1 , λ_3 and λ_4 increase while the value of λ_2 decreases. Also, the eigenvalues show scale separation, which provides the possibility of multiscale structure formation.

4. Analytical solution of the QB state

As the QB field is a linear superposition of four distinct single Beltrami fields, so the analytical solution can be expressed as

$$A = \sum_{\alpha=1}^4 C_{\alpha} F_{\alpha}, \tag{4.1}$$

where C_{α} are constants that can be calculated using appropriate boundary conditions and F_{α} is the Beltrami field satisfying the following conditions:

$$\nabla \times F_{\alpha} = \lambda_{\alpha} F_{\alpha} \dots (\text{in } \Gamma), \tag{4.2}$$

$$\mathbf{n} \cdot F_{\alpha} = 0 \dots (\text{on } \partial\Gamma), \tag{4.3}$$

where λ_{α} is a constant number either real or complex valued, $\Gamma (\subset R^3)$ is a bounded domain with a smooth boundary $\partial\Gamma$, and \mathbf{n} is the unit normal vector onto $\partial\Gamma$. Note that two important examples of Beltrami fields are the Chandrasekhar–Kendall functions in cylindrical geometry and Arnold–Beltrami–Childress fields in slab geometry (Chandrasekhar & Kendall 1957; Moffatt 1978). Here, in an axisymmetric cylindrical geometry, the Beltrami field F_{α} can be given as

$$F_{\alpha} = \begin{pmatrix} 0 \\ J_1(\lambda_{\alpha} r) \\ J_0(\lambda_{\alpha} r) \end{pmatrix}, \tag{4.4}$$

where J_0 and J_1 are Bessel functions of first kind. Now, we use the following boundary conditions to calculate the values of C_{α} : $|A_z|_{r=0} = b_1$, $|A_{\theta}|_{r=d} = b_2$, $|(\nabla \times A)_z|_{r=0} = b_3$ and $|(\nabla \times A)_{\theta}|_{r=d} = b_4$, where b_{α} and d are some real valued arbitrary constants. From

these boundary conditions, $C_\alpha = R_\alpha L^{-1}$, where

$$R_1 = J_1(d\lambda_4)[b_2\lambda_4\Lambda_4 - b_4\Lambda_4] - J_1(d\lambda_2)[\Lambda_5\Lambda_{10}J_1(d\lambda_4) + \Lambda_6\Lambda_{11}] - J_1(d\lambda_3)[\Lambda_4\Lambda_8J_1(d\lambda_2) + \Lambda_5\Lambda_7 + \Lambda_6\Lambda_9J_1(d\lambda_4)], \tag{4.5}$$

$$R_2 = J_1(d\lambda_4)[b_4\Lambda_2 - b_2\lambda_4\Lambda_2] + J_1(d\lambda_3)[\Lambda_6\Lambda_{12}J_1(d\lambda_4) - \Lambda_3\Lambda_7] + J_1(d\lambda_1)[\Lambda_2\Lambda_8J_1(d\lambda_3) - \Lambda_6\Lambda_{13} + \Lambda_3\Lambda_{10}J_1(d\lambda_4)], \tag{4.6}$$

$$R_3 = J_1(d\lambda_2)[\Lambda_3\Lambda_{11} - \Lambda_5\Lambda_{12}J_1(d\lambda_4)] + J_1(d\lambda_4)[b_2\lambda_4\Lambda_1 - b_4\Lambda_1] + J_1(d\lambda_1)[\Lambda_5\Lambda_{13} + \Lambda_3\Lambda_9J_1(d\lambda_4) - \Lambda_1\Lambda_8J_1(d\lambda_2)], \tag{4.7}$$

$$R_4 = J_1(d\lambda_2)[\Lambda_4\Lambda_{12}J_1(d\lambda_3) - \Lambda_2\Lambda_{11}] + J_1(d\lambda_3)[b_4\Lambda_1 - b_2\lambda_3\Lambda_1] - J_1(d\lambda_1)[\Lambda_4\Lambda_{13} + \Lambda_2\Lambda_9J_1(d\lambda_3) + \Lambda_1\Lambda_{10}J_1(d\lambda_2)], \tag{4.8}$$

$$L = J_1(d\lambda_3)[\Lambda_2\Lambda_5J_1(d\lambda_1) - \Lambda_1\Lambda_6J_1(d\lambda_4)] - \Lambda_3\Lambda_4J_1(d\lambda_1)J_1(d\lambda_4) + J_1(d\lambda_2)[\Lambda_2\Lambda_5J_1(d\lambda_4) - \Lambda_3\Lambda_4J_1(d\lambda_3) - \Lambda_1\Lambda_6J_1(d\lambda_1)], \tag{4.9}$$

where $\Lambda_1 = \lambda_1 - \lambda_2$, $\Lambda_2 = \lambda_1 - \lambda_3$, $\Lambda_3 = \lambda_1 - \lambda_4$, $\Lambda_4 = \lambda_2 - \lambda_3$, $\Lambda_5 = \lambda_2 - \lambda_4$, $\Lambda_6 = \lambda_3 - \lambda_4$, $\Lambda_7 = b_4 - b_2\lambda_3$, $\Lambda_8 = b_3 - b_1\lambda_4$, $\Lambda_9 = b_3 - b_1\lambda_2$, $\Lambda_{10} = b_1\lambda_3 - b_3$, $\Lambda_{11} = b_4 - b_2\lambda_2$, $\Lambda_{12} = b_3 - b_1\lambda_1$ and $\Lambda_{13} = b_2\lambda_1 - b_4$. Now by applying the relation $\mathbf{B} = \nabla \times \mathbf{A}$, the following expression can be obtained for the magnetic field:

$$\mathbf{B} = \sum_{\alpha=1}^4 \lambda_\alpha C_\alpha \begin{pmatrix} 0 \\ J_1(\lambda_\alpha r) \\ J_0(\lambda_\alpha r) \end{pmatrix}. \tag{4.10}$$

Similarly, from the (2.18), the analytical solution for composite flow V can be written as

$$V = \sum_{\alpha=1}^4 D_\alpha C_\alpha \begin{pmatrix} 0 \\ J_1(\lambda_\alpha r) \\ J_0(\lambda_\alpha r) \end{pmatrix}, \tag{4.11}$$

where $D_\alpha = d_1\lambda_\alpha^3 - d_2\lambda_\alpha^2 + d_3\lambda_\alpha - d_4$. After formulating the analytical solution for the magnetic field and flow, we will now focus on the effect of the thermal energy of plasma species for the fixed values of Beltrami parameters on the relaxed state and also on the formation of multiscale structures and their implications. As stated in the introduction, relativistic hot EP can exist in numerous astrophysical environments, including the early universe, pulsar magnetospheres and AGN. But in this study, we will work with a low-density plasma with $n = 1 \text{ cm}^{-3}$ (for which λ_e is $3.75 \times 10^5 \text{ cm}$) (Iqbal *et al.* 2008) to model large-scale structures with arbitrary values of Beltrami parameters and relativistic temperatures. In figure 3, for the given values of plasma parameters, i.e. $a = 1.0, b = 2.0, b_1 = 0.8, b_2 = 2.0, b_3 = 1.0$ and $b_4 = 0.1$, the effect of thermal energy G on the variations of the magnetic structures is illustrated. For the aforementioned plasma parameters when $G = 2$, two eigenvalues are real while the other two are complex conjugate ($\lambda_1 = 4.17 \times 10^{-18}$, $\lambda_2 = 1.89$ and $\lambda_{3,4} = 0.558 \pm 0.295i$). For this combination of real and complex eigenvalues, the relaxed state shows a diamagnetic trend. On the other hand, for an ultrarelativistic regime, such that when $G = 8$, all the eigenvalues become real, and their values are $\lambda_1 = 1.67 \times 10^{-17}$, $\lambda_2 = 0.103$, $\lambda_3 = 0.93$ and $\lambda_4 = 1.97$. Corresponding to these real-valued scale parameters, the magnetic field shows a paramagnetic trend. It is abundantly clear from this analysis that for the given

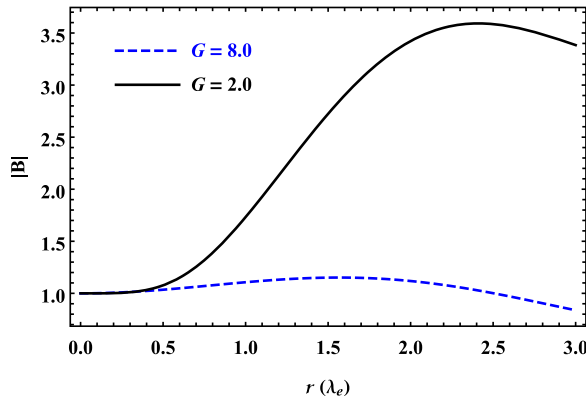


FIGURE 3. Profiles of QB magnetic field for $a = 1.0$, $b = 2.0$, $G = 2.0$ (solid) and 8.0 (dashed).

Beltrami parameters with appropriate boundary conditions, the thermal energy of plasma species can transform the behaviour of relaxed state structures.

In the subsequent discussion, we will demonstrate that the formation of multiscale structures in this QB state can create microscale kinetic or magnetic energy reservoirs. Consider the scenario when $a \approx b \gg G$, in which the values of plasma parameters are $a = 40.0$, $b = 39.7$ and $G = 8.0$. From these plasma parameters, one can obtain the following values of the scale parameters: $\lambda_1 = 4.98 \times 10^{-10}$, $\lambda_2 = 0.003$, $\lambda_3 = 39.7$ and $\lambda_4 = 39.99$. As mentioned earlier that for a photon of mass 10^{-49} g the value of λ_p is 3×10^{11} cm (Adelberger *et al.* 2007; Particle Data Group 2022) whereas for a plasma with a number density of $n = 1 \text{ cm}^{-3}$, λ_e is 3.75×10^5 cm, so the sizes of relaxed state vortices corresponding to the scale parameters are $l_1 = 7.53 \times 10^{14}$ cm, $l_2 = 1.19 \times 10^8$ cm, $l_3 = 9.45 \times 10^3$ cm and $l_4 = 9.37 \times 10^3$ cm. From these dimensions of the vortices, the existence of multiscale structures ($l_1 \gg \lambda_p$, $l_2 \gg \lambda_e$ and $l_{3,4} \ll \lambda_e$) in the QB state is evident. Next, we investigate the effect of these multiscale structures on the field and flow profiles for some suitable boundary conditions ($b_1 = 0.2$, $b_2 = 1.0$, $b_3 = 0.1$ and $b_4 = 0.3$). Figure 4 shows that the magnetic field is weak and jittery while the flow is smooth and strong. From the plot, one can also infer that the relatively small value of the magnetic field is created by the conversion of kinetic energy into magnetic energy. During this process of converting one kind of energy into another, the flow field is acting in opposition to the Lorentz force. Therefore, the presence of two microscale structures and two macroscale structures in the QB equilibrium state indicates that ambient kinetic energy dominates over magnetic energy.

Consider another case when $a \gg b$ with following values of plasma parameters and boundary conditions: $a = 20.0$, $b = 1.0$, $G = 8.0$, $b_1 = 2.0$, $b_2 = 4.0$, $b_3 = 0.11$ and $b_4 = 0.075$. The eigenvalues of the relaxed state for these plasma parameters are $\lambda_1 = 2.38 \times 10^{-11}$, $\lambda_2 = 0.07$, $\lambda_3 \approx b$ and $\lambda_4 \approx a$. Corresponding to these eigenvalues, the lengths of equilibrium state vortices are $l_1 = 1.57 \times 10^{16}$ cm, $l_2 = 5.33 \times 10^6$ cm, $l_3 = 4.02 \times 10^5$ cm and $l_4 = 1.87 \times 10^4$ cm. The scale hierarchy of these structures is $l_1 \gg \lambda_p$, $l_2 > \lambda_e$, $l_3 \sim \lambda_e$, and $l_4 < \lambda_e$. Corresponding to these multiscale structures, figure 5 illustrates that the magnetic field is strong and smooth, whereas the flow is weak and jittery. Moreover, this trend also indicates that ambient magnetic energy is higher than kinetic energy.

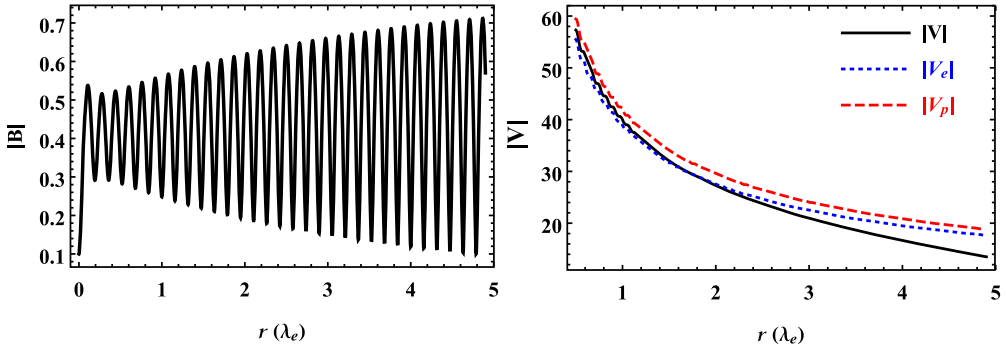


FIGURE 4. Magnetic field and flow profiles for $a = 40.0$, $b = 39.7$ and $G = 8.0$.

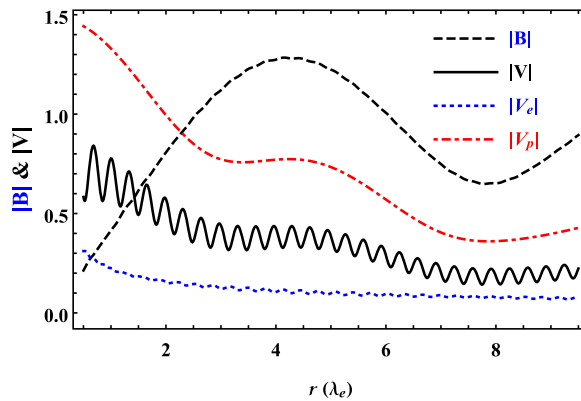


FIGURE 5. Magnetic field and flow profiles for $a = 20.0$, $b = 1.0$ and $G = 8.0$.

The role of these ambient microscale energy reservoirs in relaxed states in driving dynamo and reverse dynamo mechanisms in astrophysical plasmas has been investigated by many authors (Mininni *et al.* 2002; Mahajan *et al.* 2005; Lingam & Mahajan 2015; Kotorashvili *et al.* 2020; Kotorashvili & Shatashvili 2022). In the dynamo process, magnetic fields are generated by the motion of an electrically conducting fluid. This phenomenon is characterized by the conversion of kinetic energy into magnetic energy. On the other hand, the reverse dynamo process involves the transformation of magnetic energy into kinetic energy and the generation of flow from the magnetic field. Therefore, based on the aforementioned discussion and the values of scale parameters calculated based on the plasma parameters and photon mass, several potential implications of the current investigation can be realized. For instance, in astrophysical EP plasmas, any observational signatures of magnetic field structures larger than the Compton wavelength can be used to set an upper limit on photon mass (Ryutov 2007, 2010; Bhattacharjee 2023). Moreover, the hypothetical Maxwell–Proca stress resulting from a non-zero photon mass in the relaxed state may play a role in the comprehension of flat galactic rotation curves (Ryutov *et al.* 2019) as well as pulsar spin-down. For instance, in a recent study, Yang & Zhang (2017) devised a new method for establishing a photon mass limit by exploiting spin-down information from pulsars. In the case of AGNs, it is also possible to hypothesize that if the galactic rotation curves are flat, this could indicate that AGNs can accrete gas from a greater volume of space. This may enable them to grow faster and become more

powerful. The flatness of the curves may aid in channelling gas into the central regions of galaxies, where it may fuel the development of a supermassive black hole. Moreover, in plasmas, the microscale field and flow structures serve as energy reservoirs for driving dynamo and reverse dynamo mechanisms (Mahajan *et al.* 2005). But in the context of Maxwell–Proca electrodynamics, these kinds of studies have not been done yet. As the QB state has both large-scale and small-scale structures, the dynamo and reverse dynamo mechanisms, employing the standard methodology developed by Mahajan *et al.* (2005), can also be used in the framework of Maxwell–Proca electrodynamics in future studies.

5. Summary

The relaxed state of relativistic hot EP plasma has been investigated for the very first time by incorporating the effect of non-zero photon mass. In this study, Maxwell–Proca electrodynamics has been utilized to account for the effects of non-zero photon mass. From relativistic macroscopic evolution equations for inertial hot pair species and a modified Ampere’s law that also accounts for the inertial effect of photons, a QB relaxed state for the magnetic vector potential has been derived. The QB state is a non-force-free state that is a linear sum of four single force-free fields and is characterized by four self-organized vortices, which also show significant field and flow coupling. This QB equilibrium state can also be derived by the constrained minimization of ideal invariants of the plasma system. Based on the above-mentioned model equations, the ideal invariants of this plasma system are the generalized helicities for pair species and the magnetofluid energy. The expression for magnetofluid energy also demonstrates that due to the incorporation of the inertia of mobile fluid photons, there is a negative Maxwell–Proca stress that can pull plasmas towards a stronger magnetic field. Furthermore, the analysis of the relaxed state shows that at higher relativistic temperatures and for larger values of Beltrami parameters, all the scale parameters become real and distinct. The QB self-organized vortices also show a multiscale nature, and the inclusion of non-zero photon mass in the plasma model guarantees the existence of one self-organized structure larger than the Compton wavelength of the photons. However, any observational signatures connected to these multiscale structures can also serve as a crucial basis for refining the estimates of the upper bound on the photon mass. Additionally, the analytical solution for magnetic field and coupled plasma flow for this QB state in an axisymmetric cylindrical geometry is provided. The analysis of the field profiles shows that at lower relativistic temperatures, plasma has a diamagnetic trend for certain values of Beltrami parameters. Also, the formation of multiscale structures can create microscale reservoirs of kinetic or magnetic energy. This ambient microscale kinetic or magnetic energy has the potential to significantly contribute to the creation of macroscopic fields and flows through dynamo and reverse dynamo processes. In conclusion, the presence of QB multiscale self-organized field structures in relativistic pair plasma, within the framework of Proca electrodynamics, has the potential to contribute to the resolution of challenges such as the upper limit on photon mass and galactic rotation curves.

Acknowledgements

Editor D. Uzdensky thanks the referees for their advice in evaluating this article.

Funding

The work of M.I. is supported by Higher Education Commission (HEC), Pakistan, under project no. 20-9408/Punjab/NRPU/R&D/HEC/2017-18.

Declaration of interests

The authors report no conflict of interest.

REFERENCES

- ADELBERGER, E., DVALI, G. & GRUZINOV, A. 2007 Photon-mass bound destroyed by vortices. *Phys. Rev. Lett.* **98** (1), 010402.
- AGHANIM, N., AKRAMI, Y., ASHDOWN, M., AUMONT, J., BACCIGALUPI, C., BALLARDINI, M., BANDAY, A.J., BARREIRO, R.B., BARTOLO, N., BASAK, S., *et al.* 2020 Planck 2018 results. *Astron. Astrophys.* **641**, A6.
- ANDERSON, P.W. 1963 Plasmons, gauge invariance, and mass. *Phys. Rev.* **130** (1), 439–442.
- ASENJO, F.A. & MAHAJAN, S.M. 2019 Diamagnetic field states in cosmological plasmas. *Phys. Rev. E* **99** (5), 053204.
- BAY, Z. & WHITE, J.A. 1972 Frequency dependence of the speed of light in space. *Phys. Rev. D* **5** (4), 796–799.
- BEREZHIANI, V.I., MAHAJAN, S.M., YOSHIDA, Z. & OHASHI, M. 2002 Self-trapping of strong electromagnetic beams in relativistic plasmas. *Phys. Rev. E* **65** (4), 047402.
- BEREZHIANI, V.I., SHATASHVILI, N.L. & MAHAJAN, S.M. 2015 Beltrami–Bernoulli equilibria in plasmas with degenerate electrons. *Phys. Plasmas* **22** (2), 022902.
- BHATTACHARJEE, C. 2020 Classifying diamagnetic states of plasma near schwarzschild event horizon: local approximation. *Phys. Lett. A* **384** (27), 126698.
- BHATTACHARJEE, C. 2023 Implications of nonzero photon mass on plasma equilibria. *Phys. Rev. E* **107** (3), 035207.
- BHATTACHARJEE, C., DAS, R., STARK, D.J. & MAHAJAN, S.M. 2015 Beltrami state in black-hole accretion disk: a magnetofluid approach. *Phys. Rev. E* **92** (6), 063104.
- BHATTACHARJEE, C. & FENG, J.C. 2020 On Beltrami states near black hole event horizon. *Phys. Plasmas* **27** (7), 072901.
- BHATTACHARJEE, C., FENG, J.C. & STARK, D.J. 2018 Surveying the implications of generalized vortical dynamics in curved space–time. *Mon. Not. R. Astron. Soc.* **481** (1), 206–216.
- BHATTACHARYYA, R., JANAKI, M.S. & DASGUPTA, B. 2003 Relaxation in electron–positron plasma: a possibility. *Phys. Lett. A* **315** (1–2), 120–125.
- BHATTACHARYYA, R., JANAKI, M.S., DASGUPTA, B. & ZANK, G.P. 2007 Solar arcades as possible minimum dissipative relaxed states. *Sol. Phys.* **240** (1), 63–76.
- BJÖERNSSON, G., ABRAMOWICZ, M.A., CHEN, X. & LASOTA, J.-P. 1996 Hot accretion disks revisited. *Astrophys. J.* **467**, 99.
- BROWNING, P.K. & VAN DER LINDEN, R.A.M. 2003 Solar coronal heating by relaxation events. *Astron. Astrophys.* **400** (1), 355–367.
- CHANDRASEKHAR, S. & KENDALL, P.C. 1957 On force-free magnetic fields. *Astrophys. J.* **126**, 457.
- CURTIS, M.F. 1991 *The Theory of Neutron Stars Magnetospheres*. University of Chicago Press.
- FILIPPI, A. & DE NAPOLI, M. 2020 Searching in the dark: the hunt for the dark photon. *Rev. Phys.* **5**, 100042.
- FUENTES-FERNÁNDEZ, J., PARNELL, C.E. & HOOD, A.W. 2010 Magnetohydrodynamics dynamical relaxation of coronal magnetic fields. *Astron. Astrophys.* **514**, A90.
- GIBBONS, G.W., HAWKING, S.W. & SIKLOS, S.T.C. (Eds) 1983 *The Very Early Universe*. Cambridge University Press.
- GOLDHABER, A.S. & NIETO, M.M. 1971 Terrestrial and extraterrestrial limits on the photon mass. *Rev. Mod. Phys.* **43** (3), 277–296.
- GOLDHABER, A.S. & NIETO, M.M. 2010 Photon and graviton mass limits. *Rev. Mod. Phys.* **82** (1), 939–979.
- IQBAL, M., BERZHIANI, V.I. & YOSHIDA, Z. 2008 Multiscale structures in relativistic pair plasmas. *Phys. Plasmas* **15** (3), 032905.
- IQBAL, M. & SHUKLA, P.K. 2012 Beltrami fields in a hot electron–positron–ion plasma. *J. Plasma Phys.* **78** (3), 207–210.

- IQBAL, M. & SHUKLA, P.K. 2013 Multiscale structures in a two-temperature relativistic electron–positron–ion plasma. *J. Plasma Phys.* **79** (5), 715–720.
- ISTOMIN, Y.N. & SOBYANIN, D.N. 2007 Electron–positron plasma generation in a magnetar magnetosphere. *Astron. Lett.* **33** (10), 660–672.
- JACKSON, J.D. 2021 *Classical Electrodynamics*, 3rd edn. John Wiley & Sons.
- KAGAN, D. & MAHAJAN, S.M. 2010 Application of double Beltrami states to solar eruptions. *Mon. Not. R. Astron. Soc.* **406** (2), 1140.
- KOTORASHVILI, K., REVAZASHVILI, N. & SHATASHVILI, N.L. 2020 Dynamical fast flow generation/acceleration in dense degenerate two-fluid plasmas of astrophysical objects. *Astrophys. Space Sci.* **365** (11), 175.
- KOTORASHVILI, K. & SHATASHVILI, N.L. 2022 Macroscale fast flow and magnetic-field generation in two-temperature relativistic electron–ion plasmas of astrophysical objects. *Astrophys. Space Sci.* **367** (1), 2.
- KRISHAN, V. 2004 Magnetic fluctuations and Hall magnetohydrodynamic turbulence in the solar wind. *J. Geophys. Res.* **109** (A11), A11105.
- KRISHAN, V. & MAHAJAN, S.M. 2004 Hall-MHD turbulence in the solar atmosphere. *Sol. Phys.* **220** (1), 29–41.
- LIANG, E.P.T. 1979 Electron–positron pair production in hot unsaturated Compton accretion models around black holes. *Astrophys. J.* **234**, 1105.
- LIGHTMAN, A.P. & ZDZIARSKI, A.A. 1987 Pair production and Compton scattering in compact sources and comparison to observations of active galactic nuclei. *Astrophys. J.* **319**, 643.
- LINGAM, M. & MAHAJAN, S.M. 2015 Modelling astrophysical outflows via the unified dynamo–reverse dynamo mechanism. *Mon. Not. R. Astron. Soc. Lett.* **449** (1), L36–L40.
- MAHAJAN, S.M. & LINGAM, M. 2015 Multi-fluid systems – multi-Beltrami relaxed states and their implications. *Phys. Plasmas* **22** (9), 092123.
- MAHAJAN, S.M., MIKLASZEWSKI, R., NIKOL'SKAYA, K.I. & SHATASHVILI, N.L. 2001 Formation and primary heating of the solar corona: theory and simulation. *Phys. Plasmas* **8** (4), 1340–1357.
- MAHAJAN, S.M., SHATASHVILI, N.L., MIKELADZE, S.V. & SIGUA, K.I. 2005 Acceleration of plasma flows due to reverse dynamo mechanism. *Astrophys. J.* **634** (1), 419–425.
- MAHAJAN, S.M. & YOSHIDA, Z. 1998 Double curl Beltrami flow: diamagnetic structures. *Phys. Rev. Lett.* **81** (22), 4863–4866.
- MENDONÇA, J.T., MARTINS, A.M. & GUERREIRO, A. 2000 Field quantization in a plasma: photon mass and charge. *Phys. Rev. E* **62** (2), 2989–2991.
- MENDONÇA, J.T. & SHUKLA, P.K. 2008 Effective photon charge in relativistically hot electron–positron plasmas. *Phys. Scr.* **77** (1), 018201.
- MININNI, P.D., GÓMEZ, D.O. & MAHAJAN, S.M. 2002 Dynamo action in hall magnetohydrodynamics. *Astrophys. J.* **567** (1), L81–L83.
- MOFFATT, H.K. 1978 *Magnetic Field Generation in Electrically Conducting Fluids*. Cambridge University Press.
- OHSAKI, S., SHATASHVILI, N.L., YOSHIDA, Z. & MAHAJAN, S.M. 2002 Energy transformation mechanism in the solar atmosphere associated with magnetofluid coupling: explosive and eruptive events. *Astrophys. J.* **570** (1), 395–407.
- PARTICLE DATA GROUP 2022 Review of particle physics. *Prog. Theor. Exp. Phys.* **2022** (8), 083C01.
- PINO, J., LI, H. & MAHAJAN, S. 2010 Relaxed states in relativistic multifluid plasmas. *Phys. Plasmas* **17** (11), 112112.
- RAWLS, J.M. 1972 Pulsar data and the dispersion relation for light. *Phys. Rev. D* **5** (2), 487–489.
- REECE, M. 2019 Photon masses in the landscape and the swampland. *J. High Energy Phys.* **2019** (7), 181.
- RYUTOV, D.D. 1997 The role of finite photon mass in magnetohydrodynamics of space plasmas. *Plasma Phys. Control. Fusion* **39** (5A), A73–A82.
- RYUTOV, D.D. 2007 Using plasma physics to weigh the photon. *Plasma Phys. Control. Fusion* **49** (12B), B429–B438.
- RYUTOV, D.D. 2009 Relating the Proca photon mass and cosmic vector potential via solar wind. *Phys. Rev. Lett.* **103** (20), 201803.

- RYUTOV, D.D. 2010 Constraints on the photon mass from the galactic magnetic field structure. *AIP Conf. Proc.* **1242**, 1–10.
- RYUTOV, D.D., BUDKER, D. & FLAMBAUM, V.V. 2019 A hypothetical effect of the Maxwell–Proca electromagnetic stresses on galaxy rotation curves. *Astrophys. J.* **871** (2), 218.
- SARRI, G., PODER, K., COLE, J.M., SCHUMAKER, W., DI PIAZZA, A., REVILLE, B., DZELZAINIS, T., DORIA, D., GIZZI, L.A., GRITTANI, G., *et al.* 2015 Generation of neutral and high-density electron–positron pair plasmas in the laboratory. *Nat. Commun.* **6** (1), 6747.
- SHATASHVILI, N.L., MAHAJAN, S.M. & BEREZHIANI, V.I. 2016 Mechanisms for multi-scale structures in dense degenerate astrophysical plasmas. *Astrophys. Space Sci.* **361** (2), 70.
- SHATASHVILI, N.L., MAHAJAN, S.M. & BEREZHIANI, V.I. 2019 On the relaxed states in the mixture of degenerate and non-degenerate hot plasmas of astrophysical objects. *Astrophys. Space Sci.* **364** (9), 148.
- SHAZAD, U. & IQBAL, M. 2023 On the quadruple Beltrami fields in thermally relativistic electron–positron–ion plasma. *Phys. Scr.* **98** (5), 055605.
- SHAZAD, U., IQBAL, M. & ULLAH, S. 2021 Self-organized multiscale structures in thermally relativistic electron–positron–ion plasmas. *Phys. Scr.* **96** (12), 125627.
- SHUKLA, P.K. 1993 Non-linear coupling between electromagnetic and sound waves in relativistically hot electron–positron magnetoplasmas. *Europhys. Lett.* **22** (9), 695–699.
- SHUKLA, P.K., TSINTSADZE, N.L. & TSINTSADZE, L.N. 1993 Nonlinear interaction of photons and phonons in a relativistically hot electron–positron gas. *Phys. Fluids B* **5** (1), 233–235.
- STEINHAEUER, L.C. 2002 Double mode condensates of a flowing plasma as possible relaxed states. *Phys. Plasmas* **9** (9), 3767–3774.
- STEINHAEUER, L.C. & ISHIDA, A. 1997 Relaxation of a two-specie magnetofluid. *Phys. Rev. Lett.* **79** (18), 3423–3426.
- TAJIMA, T. & TANIUTI, T. 1990 Nonlinear interaction of photons and phonons in electron–positron plasmas. *Phys. Rev. A* **42** (6), 3587–3602.
- TAYLOR, J.B. 1974 Relaxation of toroidal plasma and generation of reverse magnetic fields. *Phys. Rev. Lett.* **33** (19), 1139–1141.
- TU, L.-C. & LUO, J. 2004 Experimental tests of Coulomb’s Law and the photon rest mass. *Metrologia* **41** (5), S136–S146.
- TU, L.-C., LUO, J. & GILLIES, G.T. 2005 The mass of the photon. *Rep. Prog. Phys.* **68** (1), 77–130.
- USOV, V.V. 1998 Bare quark matter surfaces of strange stars and e^+e^- emission. *Phys. Rev. Lett.* **80** (2), 230–233.
- WHITE, T.R. & LIGHTMAN, A.P. 1989 Hot accretion disks with electron–positron pairs. *Astrophys. J.* **340**, 1024.
- WOLTJER, L. 1958 A theorem on force-free magnetic fields. *Proc. Natl Acad. Sci.* **44** (6), 489–491.
- YANG, Y.-P. & ZHANG, B. 2017 Tight constraint on photon mass from pulsar spindown. *Astrophys. J.* **842** (1), 23.